VNU Journal of Science: Mathematics - Physics

Journal homepage: https://js.vnu.edu.vn/MaP

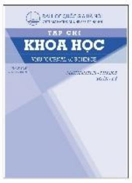

Original Article

Study on Preparation of Ag - SiO_2 Nanocomposite Material Enhancing Fluorescence for Rhodamine 6G

Bui Van Hong, Hoang Chi Hieu*, Nguyen Thi Bao Yen

VNU University of Science, 334 Nguyen Trai, Thanh Xuan, Hanoi, Vietnam

Received 8th October 2025
Revised 10th November 2025; Accepted 28th April 2026

Abstract: Ag - SiO_2 nanocomposite material was synthesized by the Stöber method and reduction process. SEM images showed that SiO_2 in the form of a nanosphere, and an average particle size of 165 nm, and Ag nanoparticles possess an average particle size of 17 nm, distributed quite evenly on the surface of SiO_2 nanospheres. The UV - Vis absorption spectrum of Ag - SiO_2 material presents a broad band at 400 nm attributed to plasmon surface resonance of Ag nanoparticles. Mixing up solutions of Ag - SiO_2 and R6G, a fluorescence band of Rhodamine 6G (R6G) at 570 nm increased 86 times compared with that of only R6G. The as-prepared Ag - SiO_2 nanocomposite material also increased the fluorescence intensity of R6G with concentration varying from 0.1 to 100 ppm.

Keywords: Ag - SiO_2, Rhodamine 6G, MEF, photoluminescence, fluorescence.

1. Introduction

SiO_2 possesses thermal stability, chemical inertness, and non-toxic properties. Moreover, the nanostructure of SiO_2 can easily be fabricated into nanoparticles and uniformly dispersed in various solutions. Due to its high biocompatibility and functionalized surface, it can readily bond with metals [1]. eanwhile, the surface plasmon resonance (SPR) of Ag nanoparticles around 400 nm, can generate enhanced fluorescence with dyes [2]. Experimental and theoretical studies have shown that enhancement fluorescence is dependent on multiple factors, such as the type, size, and shape of metal, the metal-fluorophore distance, the radiative decay rate, and the quantum yield of the fluorophore, as well as the overlap of the absorption and emission bands of the fluorophore with the metal's plasmon band [3]. Ag - SiO_2 nanostructures have been successfully synthesized through various methods, allowing control over the morphology and size of Ag - SiO_2, which in turn affects the material's Metal-Enhanced-

---

[*] Corresponding author.
E-mail address: hieuhc@hus.edu.vn

https//doi.org/10.25073/2588-1124/vnumap.5085

Fluorescence (MEF) capabilities [4]. Ag - SiO_2 material has been shown to significantly enhance the fluorescence of various dyes such as crystal violet, methylene blue, malachite green (MG), and especially Rhodamine 6G (R6G)- an organic dye widely used in industry [5]. However, a critical aspect that the previous studies have not thoroughly investigated the role of Ag concentration on the MEF ability of Ag - SiO_2 material. In this report, we study the changing amount of Ag nanoparticles attached to SiO_2nanospheres by altering the concentration of $AgNO_3$ in Ag - SiO_2 synthesis process, to investigate the MEF of Ag - SiO_2 material for Rhodamine 6G (R6G).

2. Experimental

Tetraethoxysilane $Si(OC_2H_5)_4$ (99.98%), (3-aminopropyl) trimethoxysilane $H_2N(CH_2)_3Si(OCH_3)_3$ (99.96%), silver nitrate $AgNO_3$ (99.99%), sodium borohydride ($NaBH_4$), ammonia NH_3 (25%), Rhodamine 6G (R6G), and absolute ethanol were purchased from Sigma Aldrich, China. All chemicals used were of analytical grade. Deionized (DI) water was utilized in all experiments.

SiO_2 nanospheres were synthesized by the Stöber method from tetraethyl orthosilicate (TEOS), NH_3, and absolute ethanol. The Ag-coated SiO_2 nanoparticles were synthesized through the following steps: 0.1 g of SiO_2 was dissolved in ethanol, and then 3-aminopropyl trimethoxysilane (APTMS) was added, with continuous magnetic stirring. The resulting precipitate was centrifuged and washed to obtain the white precipitate. Subsequently, 0.1 g of $AgNO_3$ was dissolved in 10 ml of water, followed by the addition of 3 ml NH_3. The above white precipitation was added to the $AgNO_3$ solution and a solution of 0.01g $NaBH_4$ in 10 ml DI water, and stirred further. The as Ag - SiO_2 solution was centrifuged, then dried at 80°C to yield Ag - SiO_2 in powder form. The Ag - SiO_2 were synthesized with concentrations of $AgNO_3$ of 0.1, 0.0125, 0.003125 mol/l (denoted as M_1, M_2, M_3).

The process to investigate the MEF of Ag - SiO_2 material for the R6G was conducted as follows: the Ag - SiO_2 solution (0.01 g/10 ml) and R6G solution (0.001 g/10 ml) were mixed together in a 3:1 volume ratio to create mixture A. Mixture A was then deposited on the Si substrate, and let them dry naturally.

The microstructure and morphology of Ag - SiO_2 material were analyzed by using X-ray diffraction (XRD) spectra obtained from the PANalytical Empyrean instrument with CuKα radiation ($\lambda = 1.54056$ Å, $2\theta = 10\div70°$) and nano scanning electron microscope Nova nanoSEM NPE199. Absorption spectra were recorded using the UV-2450 absorption spectrometer. Photoluminescence spectra were excited by 325 nm radiation from a He-Cd laser and recorded on the Spectra Pro2500i spectrometer.

3. Results and Discussion

3.1. Structure and Morphology of Ag - SiO_2 Material

Figure 1 shows the XRD patterns of Ag - SiO_2 material as varying the concentrations of $AgNO_3$, ranging from 0.1 to 0.003125 mol/l. The XRD pattern of Ag-SiO_2 using $AgNO_3$ at a concentration of 0.1 mol/l presents three diffraction peaks at 2θ angles of 38.00°, 44.24°, and 64.37°, respectively corresponding to the (110), (200), and (220) planes. These peaks are assigned to the face-centered cubic (fcc) structure of Ag [2, 8]. Additionally, a broad band near $2\theta \approx 24.5°$ indicates the presence of the amorphous structure of SiO_2 [2, 8]. As the $AgNO_3$ concentration decreases, the characteristic Ag peaks remain at nearly the same 2θ positions, but their intensities progressively decrease (Figures 1b and 1c).

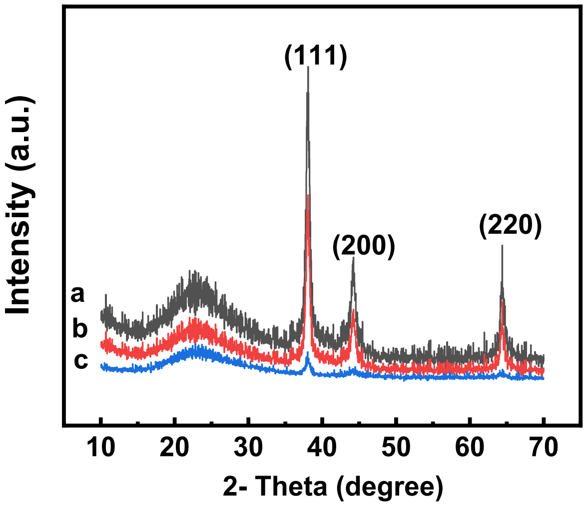

Figure 1. XRD patterns of Ag - SiO_2 material at different $AgNO_3$ concentrations: 0.1 mol/l (a), 0.0125 mol/l (b), and 0.003125 mol/l (c).

From the XRD pattern and using the Debye-Scherrer formula: $D = \frac{0.9\,\lambda}{\beta cos\theta}$ where D is the average crystallite size, λ is the X-ray wavelength (1.5406 Å), β is the full width at half maximum (FWHM) of the diffraction peak, and θ is the Bragg diffraction angle, the crystallite sizes of Ag nanoparticles at different $AgNO_3$ concentrations were calculated to be approximately 16 nm.

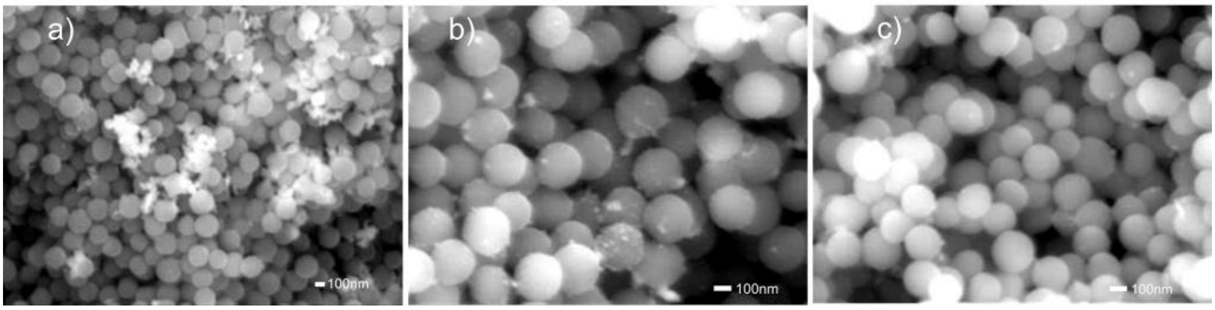

Figure 2. SEM images of Ag - SiO_2 material at different $AgNO_3$ concentrations: 0.1 mol/l (a), 0.0125 mol/l (b), and 0.003125 mol/l (c).

SEM images of Ag - SiO_2 material at varying concentrations of $AgNO_3$, from 0.1M to 0.003125M showed that Ag nanoparticles have successfully attached to the surface of the SiO_2 nanospheres. As the concentrations of $AgNO_3$ were reduced, the density of Ag nanoparticles attached to the SiO_2 surface progressively decreased.

3.2. UV-Vis Absorption Spectrum of Ag - SiO_2 Material

Figure 3 shows the UV-Vis absorption spectra of Ag - SiO_2 materials as the concentration of $AgNO_3$ was varied from 0.1 to 0.003125 M.

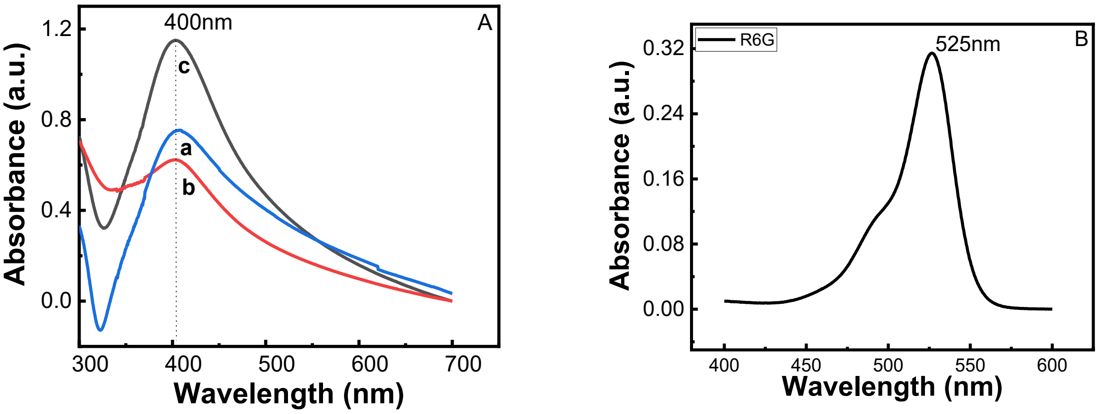

Figure 3. A. The UV-Vis absorption spectra of Ag - SiO_2 nanoparticles synthesized with varying $AgNO_3$ concentrations: M_1 (a), M_2 (b), M_3 (c) and B. The UV-Vis absorption spectrum of R6G.

The spectra display a Gaussian-like symmetrical absorption peak, indicating that Ag - SiO_2 possesses a nearly spherical shape with a narrow size distribution [6]. In sample M_1, a broad absorption band appears with a maximum at 400 nm, characteristic of the surface plasmon resonance (SPR) of Ag nanoparticles [7, 8]. When the concentration of $AgNO_3$ changes, the position of the surface plasmon absorption band of Ag remains almost unchanged, but the intensity of the band varies, as shown in Figure 3. This suggests that the $AgNO_3$ concentration affects the density of Ag nanoparticles decorating on SiO_2 nanospheres. Additionally, the UV-Vis spectrum of Rhodamine 6G (fig 3d) shows an absorption peak at 525 nm, corresponding to the monomer absorption band of R6G [9, 10].

3.3. Metal Enhanced Fluorescence Spectra of R6G Using Ag-SiO_2 Material

Figure 4 presents the MEF spectra of Ag - SiO_2 material with an $AgNO_3$ concentration of 0.0125 mol/l. The photoluminescence (PL) spectrum of Ag-SiO_2 material exhibits a weak PL peak at 430 nm, which is attributed to defects in the SiO_2 nanospheres (Figure 4a). Meanwhile, the PL spectrum of Rhodamine 6G (R6G) reveals two extremely weak peaks at 440 and 559 nm. Notably, when using Ag-SiO_2 material (M3) (Figure 4c), the 559 nm peak of R6G was enhanced by 2.4 times compared to the case without Ag - SiO_2. This demonstrates that Ag - SiO_2 effectively enhances the photoluminescence of R6G, indicating its potential application in fluorescence enhancement. The MEF effect requires a distance between the fluorophore and the metal nanostructure of about 10-20 nm. At low Ag concentrations, this distance is optimal for the most effective fluorescence enhancement. At the AgNO3 concentration of 0.003125 mol/l (M3), the distance between R6G and the Ag particles is optimal, hence generating the strongest fluorescence intensity. Excitation light interacts with the silver (Ag) nanostructures, inducing resonant oscillation of the electrons on the metal surface, thereby generating a strong local electromagnetic field around the Ag nanoparticles. When the Ag nanoparticles and R6G molecules are at an appropriate distance (10–20 nm), the emission energy of R6G is optimally enhanced due to the surface plasmon res1onance effect of Ag. SiO2 nanospheres acts as dielectric spheres that provide a stable spacing between the Ag nanoparticles and the R6G dye molecules. This ensures efficient excitation energy transfer between R6G and Ag, reaching a maximum when the AgNO3 concentration is 0.003125 mol/l.

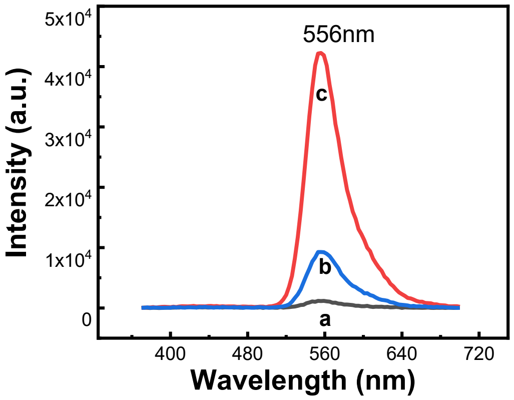

Figure 4. Fluorescence spectra of R6G when using Ag - SiO_2 material: M_1 (a), M_2 (b), M_3 (c).

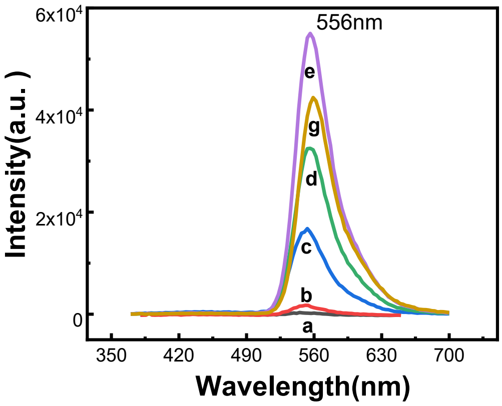

Figure 5. Fluorescence spectra of R6G using Ag - SiO_2 material at R6G concentrations of 0.1 ppm (a), 0.5 ppm (b), 1 ppm (c), 5 ppm (d), 10 ppm (e), and 100 ppm (g).

Figure 5 shows the fluorescence spectra of R6G when using Ag - SiO_2 material with the $AgNO_3$ concentration of 0.00125 mol/l at R6G concentrations ranging from 0.1 to 100 ppm. The fluorescence spectra show peaks in the range of 551-559 nm, characteristic of the R6G dye. The fluorescence intensity of R6G gradually increases as the concentration rises from 0.1 ppm to 10 ppm, reaching its maximum at 10 ppm, and then decreases at 100 ppm due to the excessively high concentration of R6G. The MEF intensity of R6G using Ag - SiO_2 increased up to 86 times compared with that of not using Ag - SiO_2. In the concentration range from 0.5 ppm to 10 ppm, the fluorescence enhancement effect is strong, but when the concentration reaches 100 ppm, the distance between R6G molecules and Ag nanoparticles becomes too long, leading to a significant reduction in fluorescence intensity. The Ag - SiO_2 material demonstrates the ability to detect and enhance the fluorescence signal of R6G even at very low concentrations, starting from just 0.1 ppm, indicating the high potential for applications in the detection of substances with high sensitivity.

4. Conclusion

The Ag - SiO_2 material was synthesized using chemical reduction and the Stöber method to enhance the fluorescence spectra of R6G dye. The synthesized Ag - SiO_2 nanocomposite material showed that Ag nanoparticles have been decorated on SiO_2 nanospheres. The Ag - SiO_2 material exhibited high quality with well-defined crystal phases, with average sizes of 24 nm and 132 nm for Ag and SiO_2, respectively. Moreover, the as-synthesized Ag - SiO_2 material was able to detect R6G at concentrations ranging from 100 to 0.1 ppm. Using this approach, the fluorescence intensity of R6G at a concentration of 10 ppm increased to 86 times compared with that of only R6G dye.

References

[1] J. R. Lakowicz, Radiative Decay Engineering: Biophysical and Biomedical Applications: Anal Biochem, Vol. 298, No. 1, 2001, pp. 1-24, https://doi.org/10.1006/abio.2001.5377.

[2] Y. Zhu, K. Morisato, W. Li, K. Kanamori, K. Nakanishi, Synthesis of Silver Nanoparticles Confined in Hierarchically Porous Monolithic Silica: A New Function in Aromatic Hydrocarbon Separations: ACS Appl Mater Interfaces, Vol. 5, No. 6, 2013, pp. 2118-2125, https://doi.org/10.1021/am303163s.

[3] J. R. Lakowicz, Plasmonics in Biology and Plasmon-Controlled Fluorescence: Plasmonics, Vol. 1, No. 1, 2006, pp. 5-33, https://doi.org/10.1007/s11468-005-9002-3.

[4] M. J. Ahemad, Y. T. Yu, Investigating the Mechanism of Uniform Ag@SiO_2 Core-shell Nanostructures Synthesis by a One-pot Sol–gel Method: J Solgel Sci Technol, Vol. 96, No. 3, 2020, pp. 679-689, https://doi.org/10.1007/s10971-020-05392-y.

[5] Y. Wang, X. Wang, W. Ma, R. Lu, W. Zhou, H. Gao, Recent Developments in Rhodamine-Based Chemosensors: A Review of The Years 2018-2022: Chemosensors 2022, Vol. 10, No. 10, 2022, pp. 399, https://doi.org/10.3390/chemosensors10100399.

[6] T. Taib, M. R. Johan, W. J. Basirun, Plasmonic SERS Active Nanostructured Ag–SiO2 at Optimum Volume Ratio Synthesized Via Sol-gel Technique: Physica B Condens Matter, Vol. 606, 2021, pp. 412638, https://doi.org/10.1016/j.physb.2020.412638.

[7] N. B. Basosila et al, Biogenic Synthesis, Spectroscopic Characterization and Bioactivity of Cymbopogon Citratus Derived Silver Nanoparticles: Journal of Applied Sciences and Nanotechnology, Vol. 3, No. 4, 2023, pp. 33-41, https://doi.org/10.53293/jasn.2023.7012.1226.

[8] D. V. Thai, P. V. Ben, S. C. Doanh, N. T. H. Giang, T. T. Duc, N. T. Dai, B. V. Hong, Synthesis of SiO_2@Ag Nanocomposite for Enhancing Photoluminescence and Raman Characterizations, 2023, https://doi.org/10.21203/rs.3.rs-3660171/v1.

[9] N. Pantelić, C. J. Seliskar, Dynamics of Rhodamine 6G Sorption into a Porous Tri-block Copolymer Thin Film: Journal of Physical Chemistry *C*, Vol. 111, No. 50, 2007, pp. 18595-18604, https://doi.org/10.1021/jp076274r.

[10] M. F. H. A. Kadhemy, K. N. Abbas, W. B. Abdalmuhdi, Physical Properties of Rhodamine 6G Laser Dye Combined in Polyvinyl Alcohol Films as Heat Sensor, IOP Conference Series, Materials Science and Engineering, 2020, pp. 928 - 072126.